A Thesis

on

SYNTHESIS AND CHARACTERIZATION OF COBALT FERRITE NANOPARTICLES

Submitted in partial fulfillment of the requirement for the award of the degree of

Master of Science

in

Physics

Submitted by

NITIKA RANI

ROLL No. 301404017

Under the supervision of

Dr. B.N.CHUDASAMA

ASSOCIATE PROFESSOR

School of Physics and Material Science

Thapar University, Patiala 147004

July 2016

Dedicated to

my

Parents

&

Brothers Naveen Garg and Prince Garg

Certificate

This is to certify that **Ms. NITIKA RANI**, Roll No. **301404017** has worked on this thesis report entitled **"SYNTHESIS AND CHARACTERIZATION OF COBALT FERRITE NANOPARTICLES"** in partial fulfillment for award of the degree of MASTER ofSCIENCE in PHYSICS in THAPAR INIVERSITY, PATIALA was carried out by her under my supervision. She has not submitted this material for credit towards any other degree at Thapar University, Patiala or any other University.

Date: 15-7-2016

Nitika Rani
NITIKA RANI
Roll No. 301404017

B. N. Chudasama
Dr. B. N. Chudasama

Associate Professor& Supervisor
School of Physics and Material Science
Thapar University, Patiala

Countersigned By:

Dr. Manoj Sharma
Professor and Head
School of Physics and Material Science
Thapar University, Patiala

Dr. S. S. Bhatia
Dean of Academic Affair
Thapar University, Patiala

Acknowledgement

Completion of my thesis is possible with the support of several people. Firstly, I would like to express my sincere appreciation and gratitude to my supervisor Dr. B. N. Chudasama, Associate professor, School of Physics and Material Science, Thapar University, Patiala, for his valuable guidance, constant encouragement during my research. He is always willing to listen, discuss and advice throughout the work. His support and inspiring suggestions have been precious for the development of this thesis content.

I also thank to Dr. Manoj Sharma, Professor and Head, School of Physics and Material Science, for his support and for providing me infrastructural facilities to conduct this research.

I would like to thank Ms. Navjot Kaur, Mrs. Parveer Kaur, Ms. Poornima, research scholars for the help provided by them. This dissertation would not have been possible without their support and discussions.

I thank to my all friends for havinggroup studies, discussions on projects and preparation of exams. I would like to thank my friend Pardeep Kaur and Alice Goyal to correct my thesis mistakes and I never felt alone in lab with her. Special thank to my friend for being with me in the thick and thins of my life and for supporting and inspiring me to complete my post graduation and thesis work. I found myself lucky to have friends like them in my life.

I owe more than thanks to my family members which includes my parents, grandparents and my siblings, for their support and encouragement throughout my life. Words cannot express how grateful I am to my mother, father for their love, prayers, caring and sacrifices for educating and preparing me for my future. Finally, I thank almighty God for giving me power to follow the right direction in achievement of my goal.

Ms. NITIKA RANI

ABSTRACT

Cobalt Ferrite nanoparticles are synthesized by using co-precipitation method.Effect of reaction pH, reaction time and reaction temperature on the structure and magnetic properties measurement of Cobalt ferrite has been studied in this thesis.As synthesized nanoparticles characterized by X-ray Diffraction (XRD), transmission electron microscope (TEM), vibrating sample magnetometer (VSM) and differential scanning calorimetry (DSC). The average crystallite size of Cobalt Ferrite nanoparticles determined from XRD analysis is found in the range of 8 to 14 nm. Each nanoparticles possesses inverse spinel structure. The saturation magnetization (M_s), Coercivity (H_c) and remanance (M_r) of nanoparticles are also determined. Saturation magnetization is of the order 15 to 35 emu/g, Coercivity is 235 to 642 Oe and remanence is 2 to 9 emu/g, which are much lower as compared to their bulk counter parts showing the effects induced by quantum confinement of electrons.An estimation of Curie point has also been done by DSC measurement which ranges from 307 to 350 °C. The physical size is 11.49 nm determined from TEM. Cobalt Ferrite nanoparticles have inverse spinel structure.

CONTENTS

List of Figures

List of Tables

Chapter 1

Introduction

1.1 Nanotechnology

Nanoparticles research has recently become an important field and widely used in material science. Nanotechnology is the study on the nanometer scale which manipulates matter at atomic scale, molecular and macromolecular scale to design objects on nanoscale [1]. Nanotechnology deals with the objects which lie in the range of 1 to 100 nm scale. The word nano derives from Greek word nano which means very small particles [2].

The properties change when nanoscale is reached. Nanoparticles are different than the bulk materials as they exhibit different properties as compared to bulk. As an example of silver, silver in bulk is non-toxic but nanoparticles of silver are capable of killing viruses [1]. Opaque materials become transparent of nanosize, bulk copper and gold particles are insoluble whereas gold nanoparticles are soluble. When particles are prepared at small scale their physical, chemical and biological properties changed [3]. Nanoparticles are widely used due to size dependent properties such as physical, chemical, biological, optical, electronic and magnetic, which arise due to large surface to volume ratio change and quantum confinement effects. Nanoparticles are being used in many applications like electronics, water filters, drug delivery applications, cancer detection and treatment, etc.

1.2 Magnetism

The magnetic materials are those materials which are attracted towards applied magnetic field. When magnetic field is applied it produces magnetization. The term magnetization is defined as magnetic moment per unit volume. The magnetic particles are classified due to their properties in five types:

1.3 Types of Magnetism

1. Diamagnetic

2. Paramagnetic

3. Ferromagnetic

4. Antiferromagnetic

5. Ferrimagnetic.

1.3.1 Diamagnetism

Diamagnetism is exhibited by all the materials. The materials have net zero atomic magnetic moment before applying the magnetic field. When a material is placed in magnetic field, the electrons start to align in the opposite direction of the applied field. Due to opposite direction the material gets repelled in the magnetic field. Susceptibility of diamagnetic materials is negative. The atoms having no permanent magnetic moment exhibit diamagnetism [4].

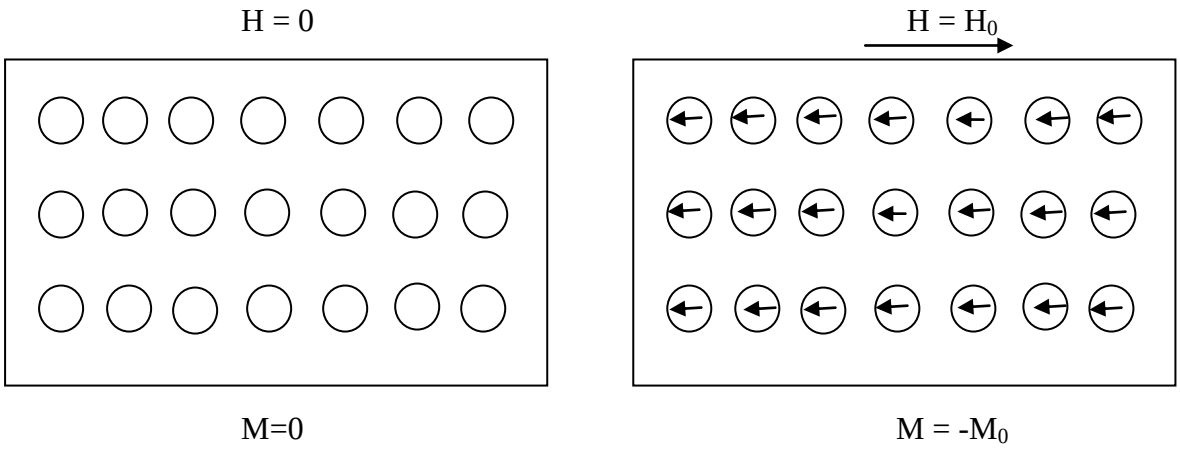

Figure 1.1: Schematic representation of induced dipole moment in diamagnetic material

1.3.2. Paramagnetism

In this material, atoms or molecules have permanently magnetized. In the absence of applied field this magnetic moments are randomly oriented and hence net magnetic moment of the solid is zero. When magnetic field is applied, the magnetic moment tends to align them in the direction of external magnetic field and due to this, net non zero magnetic moment is observed [4].

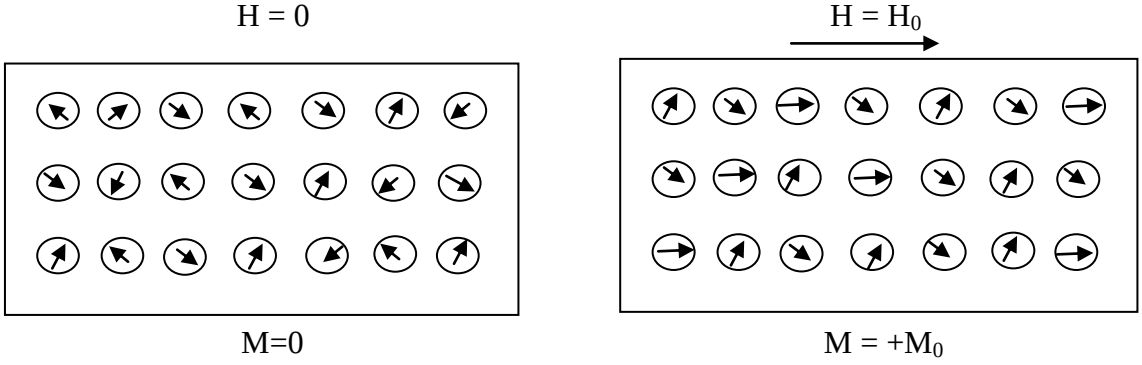

Figure 1.2: Schematic representation of behavior of dipole moments in a paramagnetic solid

1.3.3. Ferromagnetism

The materials can possess permanent magnetization. In these materials the magnetic moment are already aligned in the absence of external magnetic field. In the absence of field, the magnetic moments are aligned means that there exist internal field. Due to the presence of this external field, they get strongly attracted towards the magnetic field. Susceptibility of the ferromagnetic materials is positive [4].

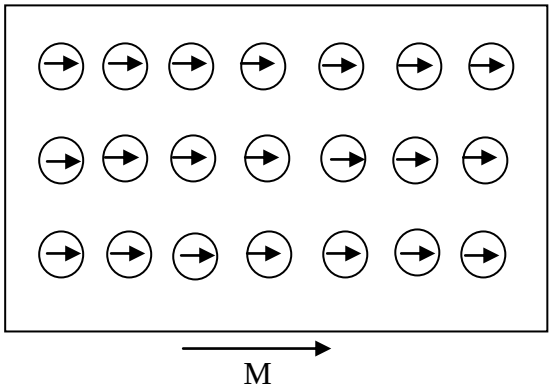

Figure 1.3: Schematic representation of spontaneous alignment of dipole moments in applied magnetic field

1.3.4. Antiferromagnetism

Antiferromagnets possess no net magnetization in the absence of magnetic field. The atoms have positive susceptibility but the value is very small. In the absence of applied field, they have no net magnetization as each of the total magnetic moment aligns in two opposite directions. In the presence of field, they get opposite magnetic moment at alternate atoms. Antiferromagnetism occurs below a critical temperature called Neel temperature. Above this the material changed to paramagnetism [4].

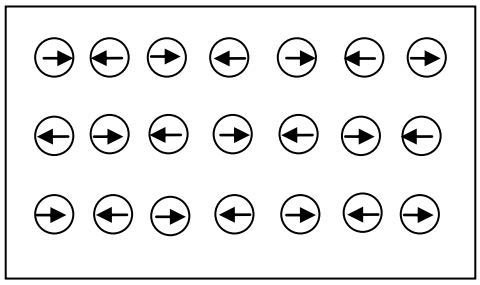

M=0

Figure 1.4: Schematic representation of spontaneous alignment of magnetic moments in the absence of external magnetic field along two directions

1.3.5. Ferrimagnetism

In ferrimagnetism, 'A' atoms are aligned in one direction and 'B' atoms are aligned in opposite direction. Unlike antiferromagnetism their magnitude is different in ferrimagnetism. Magnitude of magnetic moment of atom B is greater than magnetic moment of atom A. So the net magnetic moment can't be canceled. They exhibit magnetic behavior below critical temperature is called Curie temperature. After this temperature it changes to paramagnetism [4].

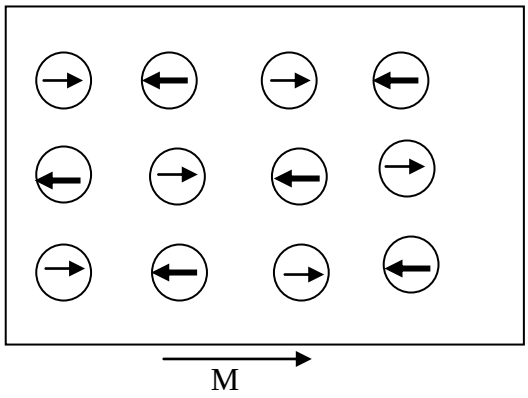

Figure 1.5: Schematic representation of magnetic moments in a ferrimagnetic substance in external magnetic field

1.4 Magnetic nanoparticles

Magnetic nanoparticles are used in diverse applications due to their unique properties which are different than that of bulk materials. The classification of magnetic properties of material depends on magnetic susceptibility, where susceptibility is defined as the ratio of induced magnetization to the applied magnetic field. When magnetic moments align parallel to the applied magnetic field, coupling interaction between electrons of material shows ordered magnetic states. The term susceptibility depends on temperature, external field and atomic structures. Small size magnetic particles become single domain and maintain large magnetic moment. Below critical size of particles, magnetic nanoparticles show interesting behavior.

Magnetic nanoparticles are commonly used in magnetic fluids, data storage and biotechnology. Magnetic nanoparticles are prepared by various methods and their properties highly dependent on which method is used to make nanoparticles [5].

1.5 Magnetism at Nanoscale

The magnetic properties at nanoscale differ basically from the bulk particles. Nanotechnology designs particles at very small scale of the order of 100 nm or even less than 100 nm whereas bulk particles are designed at micro level or larger than this.

When size is changed from micro to nanoscale the physical and chemical properties are changed. Due to these properties nanoparticles are of great interest in material science. The properties at nanoscale are different from bulk due to two effects known as surface effects and finite size effects [6].

1.5.1 Surface Effects

With decrease in particle size number of particles on surface will increase. Due to this, surface effects and interface effects become more important. For example, Cobalt particles with face centered cubic (FCC) structure of diameter approximately 1.6 nm having 60% of total atoms on surface. Hence, the contribution of surface spins becomes more important to determine magnetization of nanoparticles [7, 8].

1.5.2 Finite Size Effects

There are two commonly effects which are studied in nanoparticles. The effects are known as single domain limit and super paramagnetic limit. When particle size is very large there exist domains which are separated by domain walls. If we reduce the size of material then there is a critical volume below which it takes more energy to originate a domain wall compared to support the external magnetostatic energy of the single domain. Domain is the small field in which all the spins are ordered in one direction. For a certain direction of magnetic moment, Magnetic anisotropy energy per particle is responsible for a certain direction of magnetic moment, which is expressed as $E(\theta) = K_{eff}VSin^2\theta$, where V is volume of particle, K_{eff} is anisotropy constant [7].

1.6 Superparamagnetism

Superparamagnetism is the state of very small single domain non interacting ferromagnetic/ferrimagnetic grains where in thermal agitations is sufficient to disrupt spontaneous alignment of magnetic moments [9]. Superparamagnetism is the form of magnetism, which shows up by the ferromagnetic and ferrimagnetic nanoparticles. Below a Curie or Neel temperature, superparamagnetism exhibit behavior as paramagnetic. Superparamagnetism occurs when size of crystallite sample is very small i.e. generally in the range of 1-10 nm and have short relaxation time [10]. Due to these properties superparamagnetic nanoparticles are used in medical applications like MRI, drug delivery, magnetic hyperthermia etc. [11].

1.7 Properties of Magnetic Nanoparticles

1.7.1 Saturation Magnetization

Saturation magnetization is defined as the maximum value of magnetization w.r.t. applied field. Saturation magnetization depends on strength of dipole moment of the atoms and also depends on how densely the atoms are packed. Saturation magnetization will change with temperature. Saturation magnetization is denoted as M_s and measured in emu/g [12].

1.7.2 Coercivity

Coercivity is defined as the amount of magnetic field needed to reduce the value of magnetization of the sample to zero. The field applied to reduce the magnetization is called coercive field. Coercivity is denoted as H_c and measured in Oe [12].

1.7.3 Remanence

Remanence is the magnetization of the sample after removal of applied external field. Remanence is denoted as M_r and measured in emu/g [12].

1.8 Ferrites

Ferrites are those ceramic compounds that consist of iron oxide and one or more other metals in chemical combination [13]. The molecular formula of ferrites is $M^{2+}OFe^{3+}{}_2O_3$ where M stands for divalent metal like Fe, Mn, Co, Ni, Cd, Mg, Zn, Cu. Ferrites are the metal oxide which contains magnetic ions grouped in such a manner that it produces spontaneous magnetization [14].Ferrites are chemically stable and show high electrical resistivity. Due to high chemical stability, ferrite materials exhibit interesting properties such as optical, electrical, chemical and magnetic [15]. Ferrites are the insulating magnetic material which offers high electrical resistivity, low eddy current, high magnetic permeability, low dielectric losses, high saturation magnetization and reasonable permittivity. Ferrites are used in diverse applications because of these properties. Ferrites have high Curie temperature [16].

1.9 Applications

Ferrites are used in magnetic recording media, permanent magnets, memory chips, antenna rods, transformer cores, microwave and computer technology [17]. Ferrites can be used in drug delivery, magnetic resonance imaging, gas sensors, magnetic fluids, actuators, etc. [18]. Ferrites are used as transformers and in magnetic refrigeration [19, 20].

1.10 Classification of Ferrites

According their magnetization ferrites can be divided into two types namely soft ferrites and hard ferrites.

1.10.1 Soft ferrites

Soft ferrites have low coercivity, high saturation magnetization, low remanant magnetization, due to higher resistivity eddy current loss is very less, high permeability and high susceptibility. Soft ferrites can be easily magnetized and demagnetized, hence not suitable for permanent magnets. The hysteresis curve of soft ferrites is thin and long. Soft ferrites are iron, cobalt and manganese and these are used in electronic industry to make ferrite core for transformer and inductor and in microwave components [12, 21].

1.10.2 Hard ferrites

Hard ferrites have high coercivity, high remnant magnetization, low saturation magnetization. Hard ferrites are difficult to magnetize and demagnetize means when they are magnetized then they are difficult to demagnetize. Because of this, they are used to make permanently magnet. Hard ferrites are used in refrigerators, loudspeakers, electric motors, automobiles, air crafts, etc. [12, 21].

1.11 Structure of ferrites

1.11.1 Spinel ferrites

Spinel ferrites are also named as cubic ferrites. They are commonly used at microwave frequencies because of high electrical resistivity and low eddy current losses. Chemical formula of spinel ferrites reported as MFe_2O_4 . The unit cell of spinel ferrites is FCC with eight formula in per unit cell. So the formula can be written as $M_8Fe_{16}O_{32}$. The spinel ferrites has been classified as three categories namely normal spinel, inverse and intermediate spinel. This classification is based on cationic distribution on tetrahedral and octahedral sites [22, 23].

a) Normal Spinel

In normal spinel structure, octahedral site is occupied by one type of cation. Tetrahedral site is occupied by divalent cation while the octahedral site is occupied by trivalent cation. The formula of normal ferrites is $M^{2+}M^{3+}{}_2O_4$. Where M^{2+} is divalent metal e.g. cobalt which occupy the position at tetrahedral sites and M^{3+} is trivalent metal e.g. iron which occupy the position at octahedral sites [24].

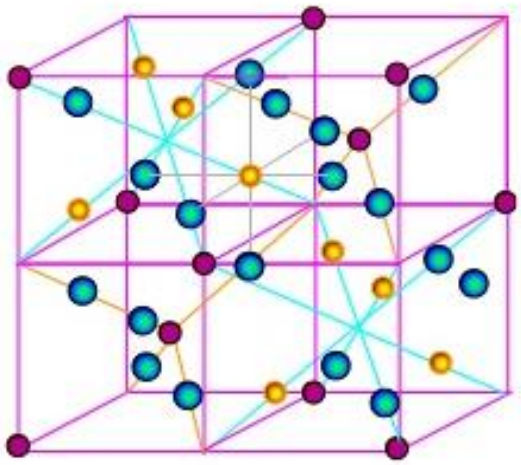

Figure 1.6: Crystal structure of spinel ferrites where purple atoms are cobalt, yellow are iron and blue are oxygen

b) Inverse Spinel

In an inverse spinel structure of ferrite nanoparticles, tetrahedral sites are occupied by half of the trivalent ions and octahedral sites are occupied by half of the trivalent and divalent ions. The formula of inverse spinel structure is $M^{3+}M^{2+}M^{3+}O_4$, where M^{2+} is divalent metal e.g. cobalt which capture the octahedral sites and M^{3+} is trivalent metal e.g. iron which occupy tetrahedral and octahedral sites equally [25, 26].

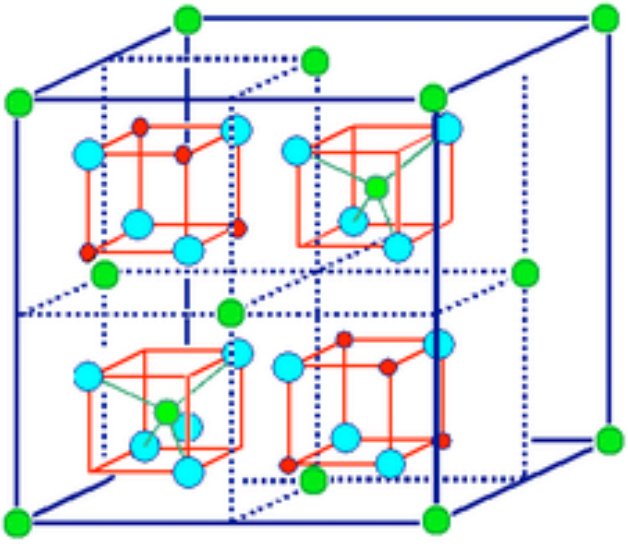

Figure 1.7: Crystal structure of inverse spinel ferrites where red atoms are octahedral sites, green are tetrahedral and blue are oxygen

c) Intermediate Spinel

Intermediate spinel structures are random spinels. The divalent and trivalent cations are randomly distributed on tetrahedral and octahedral sites. Random structures lie between normal spinel and random spinel. There is unequal number of cation on octahedral sites [27].

1.11.2 Hexagonal Ferrites

Hexagonal ferrite lattice structure is identical to cubic lattice structure with oxygen ions which are closely packed, metal ions present at intermediate layers which have ionic radii that is similar to oxygen ions. The formula of hexagonal ferrites is $MFe_{12}O_{19,}$ where M is divalent metal, Fe is iron and O is oxygen ions. Hexagonal ferrites have high coercivity and used as permanent magnets at high frequency.

1.12 Cobalt Ferrites

Cobalt ferrite nanoparticles have high coercivity and moderate saturation magnetization [28].Cobalt ferrite nanoparticles have been widely used in many applications due to high electromagnetic properties, good chemical stability and mechanical hardness. Due to these properties of cobalt ferrites are used in video and audio tapes, high density digital recording media in spintronics, solar cells, sensors and catalysis [29]. Cobalt ferrites are used as application in magnetic resonance imaging (MRI), magnetic fluid hyperthermia (MFH), biosensors, ferrofluids, magnetic separations, storage magnetic materials, targeted and controlled drug delivery [25, 26].

Saturation magnetization (M_s) of cobalt ferrite nanoparticles is smaller than that of the bulk and M_s decreasing with decrease in size. When the crystallite size is approximately equal to the single domain size then the coercivity reaches to its maximum value.

Cobalt ferrite nanoparticles have an inverse spinel structure. In this O^{2-} form FCC close packing, and Co^{2+} and Fe^{3+} occupy either tetrahedral or octahedral interstitial sites. In this inverse spinel cobalt ferrite structure half of Fe^{3+} ion and Co^{2+} ions occupy the octahedral sites and rest of Fe^{3+} ions occupy the tetrahedral sites.

Chapter 2

Literature Review

Kim et al. [2003] synthesized magnetic cobalt ferrite nanoparticles by temperature controlled co-precipitation method. It was observed that size and magnetic behavior depend on pH, salt concentration, temperature, stirring speed of the solution. Samples were prepared at 20-80 °C. It was found that samples show broad and unresolved peaks at 20°C and 40°C while the clear pattern at 60°C and 80°C corresponding to cubic, spinel type lattice was observed. The physical size was lying in between 2-15 nm and saturation magnetization was in the range of 2.0-58.3 emu/g. Both particle size and saturation magnetization (M_s) increases with increase in synthesis temperature [30].

Hanh et al. [2003] synthesized cobalt ferrite nanocrystallites by the forced hydrolysis method. Nanoparticles show ferrimagnetic behavior with high remanance and non zero coercivity. At 5 K saturation magnetization was 75 emu/g and coercivity was 10 kOe [31].

Choi et al. [2003] synthesized cobalt ferrite nanoparticles by microemulsion method. The bulk cobalt ferrite particles have high coercivity and moderate saturation magnetization. The coercivity was 5400 Oe and saturation magnetization at 5 K and at 300 K were 93.9 emu/g and 80.8 emu/g respectively. [32].

Chinnasamy et al. [2003] has worked on synthesis of cobalt ferrite nanoparticles by oxidation process. Cobalt ferrite nanoparticles were spherical in shape having diameter ranging from few micrometers to 100 nanometers. It was observed that cobalt ferrites does not obey particular trend with Fe^{3+} concentration. In this work, particular trend was not observed in size and magnetic properties of cobalt ferrite nanoparticles [33].

Maaz et al. [2007] synthesized metal oxide nanoparticles by wet chemical method. He observed that slow mixing of sodium hydroxide results into large particle size. The average particle size of calcined samples at 600 °C varies from 15 - 21 nm. The particle size increase when annealed at 800 - 1000 °C. The saturation magnetization and remanent magnetization was 68 emu/g and 31.7 emu/g at room temperature [20].

Zhao et al. [2008] prepared cobalt ferrite nanoparticles by hydrothermal method. Particles were synthesized by changing the reaction temp and time parameters. High saturation magnetization of Cobalt Ferrite nanoparticles (113emu/g) and moderate coercivity (1438Oe) was observed. [34].

Toksha et al. [2008] prepared cobalt ferrite nanoparticles by sol - gel auto combustion method. The inverse spinel structured particles with average size of 15 nm and lattice constant of 8.373 Å was observed. Saturation magnetization and coercivity at room temperature were 67 emu/g and 1215 Oe and at 77 K they were 43 emu/g and 10.2 kOe respectively. The remanance at room temperature and at 77 K was 30.2 emu/g and 35 emu/g respectively. With the increase in annealing temperature and time, the size of nanoparticles increases [35].

Zi et al. [2009] synthesized Cobalt Ferrite nanoparticles by chemical co-precipitation method. The average crystallite size of particles was 8.56 nm. The saturation magnetization of nanoparticles was 61.77 emu/g and the remanence was 14.39 emu/g at room temperature. Coercive field was 0.519 kOe [29].

Vilar et al. [2009] prepared cobalt ferrite nanoparticles by solvothermal method. The particles prepared at 180°C, 190°C heating for 24h and 48h, simultaneously. The particle size was 7.6 nm when heating for 24h at 180°C and 8.9 nm when heating for 48h at 180°C. When particles were heated for 24h at 190°C, the crystallite size was 7.1 nm. The saturation magnetization in the range of 55 to 58 emu/g and it was observed that saturation magnetization decreases when particle size decrease [36].

Zhang et al. [2010] prepared cobalt ferrite nanoparticles by co-precipitation method. These particles were heated at 95°C for 2h. Samples were prepared at different concentration of NaOH. Crystallite size of Cobalt increases with increase the concentration of NaOH. When the crystallite size is near the single domain size then the coercivity reaches to maximum. Saturation magnetization was found to decrease with the increase in particle sizes with increasing the concentration of sodium hydroxide [28].

Mohamed et al. [2010] prepared cobalt ferrite nanoparticles by organic acid precursor method. A series of experiments have been performed at many temperatures from 400 to 1000°C. It was found that with the increase in temperature, the crystallinity of samples also increases. It was observed that saturation magnetization increases with temperature and time while coercivity increases with temperature but decreases with time [37].

Okr et al. [2011] synthesized cobalt ferrite with co-precipitation method. The samples were prepared at 20 - 80 °C temperature. The sample prepared at 60°C was further annealed at temperature 500 - 900 °C for 2h and at these temperatures the average crystallite size were in the range of 9.4 - 42.3 nm. The saturation magnetization, coercivity and remanance magnetization increases with increase in annealing temperature. [38].

Sharifi et al. [2012] synthesized cobalt ferrite nanoparticles ($CoFe_2O_4$ NPs) by co-precipitation method, normal micelles method and reverse micelles method. Magnetic properties were strongly effected by crystallite size and the degree of crystallinity. Higher crystallinity in co-precipitation sample might be an additional contributing factor in the saturation magnetization. Magnetic properties of cobalt particles were lightly dependent on the distribution of cation between sites A and B and depend appreciably on particle size [25].

Briceno et al. [2012] synthesized cobalt ferrite nanoparticles using precipitation in water solution with polyethylene glycol as surfactant. Samples were prepared at 180°C for 6h at different pH in the range of 6 - 12. No specific trend in magnetic properties has been observed as a function of synthesis parameter [39].

Mazario et al. [2012] synthesized cobalt ferrite nanoparticles by electrochemical method. It was found that by changing parameters such as temperature and time. The structure of the particles was inverse spinel. Saturation magnetization and coercivity were 74 emu/g and 823 Oe respectively at high temperature and 85 emu/g and 6386 Oe at room temperature. It was observed that magnetic properties increase with increase in temperature [40].

M.Houshiar et al. [2014] synthesized cobalt ferrite nanoparticles by various methods i.e. combustion method, co-precipitation method and precipitation method. pH level was set at 12. Crystal structure was found to be inverse cubic spinel type. H_c and M_s were found to be highest in combustion process [12].

Huixia et al. [2014] prepared cobalt ferrite nanoparticles by reverse co-precipitation method. Particles were prepared at different pH and aging temperature. It was concluded that the particle size increased with aging temperature and saturation magnetization did not exhibit particular trend [41].

Hedayati et al. [2016] synthesized cobalt ferrite nanoparticles by chemical precipitation method. Magnetic properties of the sample measured at room temperature have shown that the sample exhibit superparamagnetism. The saturation magnetization (M_s) of sample was 5.4 emu/g and coercivity was very small even less than 5 Oe. After heating, it showed ferromagnetism with M_s 32 emu/g and coercivity 150 Oe [42].

From the literature survey, it has been found that no systematic trend in the structural and magnetic properties of cobalt ferrite nanoparticles has been observed. Properties of cobalt ferrite nanoparticles are different when prepared by different methods as well as when prepared under different reaction conditions. Most of the synthesis routes involved a secondary annealing step that results into larger particle size and broad size distribution of nanoparticles with increases remanance and coercivity,

which is not encouraging for most of the industrial applications of cobalt ferrite nanoparticles. Amongst the synthesis routes explored for cobalt ferrite nanoparticle synthesis, chemical co-precipitation is a rapid, easy and economical process. However, the exact role of various synthesis variables and its correlation with structural and magnetic properties of nanoparticles is not well understood in literature. Hence, in this thesis report we aimed to synthesize cobalt ferrite nanoparticles as a function of reaction pH, reaction temperature and reaction time. The correlation between this variable and their structural and magnetic properties will be established.

Chapter 3

Experimental procedure

3.1 Synthesis of cobalt ferrite nanoparticles

Materials: The reagents cobaltous acetate extrapure ($C_4H_6CoO_4.4H_2O$), iron chloride ($FeCl_3$) and sodium hydroxide were used for the synthesis of cobalt ferrite nanoparticles. Acetone is purchased from Merck India. All aqueous solutions were prepared in Milli-Q ultrapure distilled water.

Preparation: Cobalt ferrite nanoparticles were synthesized by co-precipitation method using Cobaltous acetate ($C_4H_6CoO_4.4H_2O$) and iron chloride ($FeCl_3$). The synthesis protocols are summarized in Figure 3.1. In this process sodium hydroxide (NaOH) was used as base. 10 mM of cobaltous acetate (2.49g) was dissolved in 100mL water to this. 20mM solution of iron chloride (10 mL) was added. 80 mM of 100 mL sodium hydroxide solution was also prepared. Both acid solutions when mixed and pH was adjusted below 2 with dilute HCl. Then color of solution was changes from light red to brown. To this sodium hydroxide solution was added drop by drop at series of samples were prepared by changing parameters such as reaction pH (11, 12, 13), reaction heating (25 °C, 80 °C) and time (1h, 2h). The solution pH was adjusted to desired value with excess 0.1 M NaOH solution. The reaction was allowed to proceed for 20 mins under constant mechanical stirring. During this time metal hydroxides were found which were further subject to room temperature or high temperature. Annealing for 1h or 2h. Once this annealing period gets over, it was cooled, magnetically decanted and washed with warm distilled water several times. It was then subject an acetone wash and dried at 80 °C overnight in oven. As synthesized nanoparticles were then grinded with the help of mortar pestle and presented for further characterization. Synthesis protocols followed in the entire exercise is summarized in figure 3.1.

The following reaction took place

10 mM $C_4H_6CoO_4.4H_2O$ + 80 mM NaOH + 20 mM $FeCl_3$ ⟶ 10 mM $CoFe_2O_4$ + 8 mM H_2O

3.2 Characterization

Crystal structure and average crystalline size of the nanoparticles is determined by X-Ray Diffraction (XRD). Physical size and morphology of the particles is determined by Transmission Electron Microscope (TEM). The magnetic properties like saturation magnetization (M_s), coercivity field (H_c) and remanant magnetization (M_r) is

investigated by Vibrating Sample Magnetometer. The Curie point is determined by DSC.

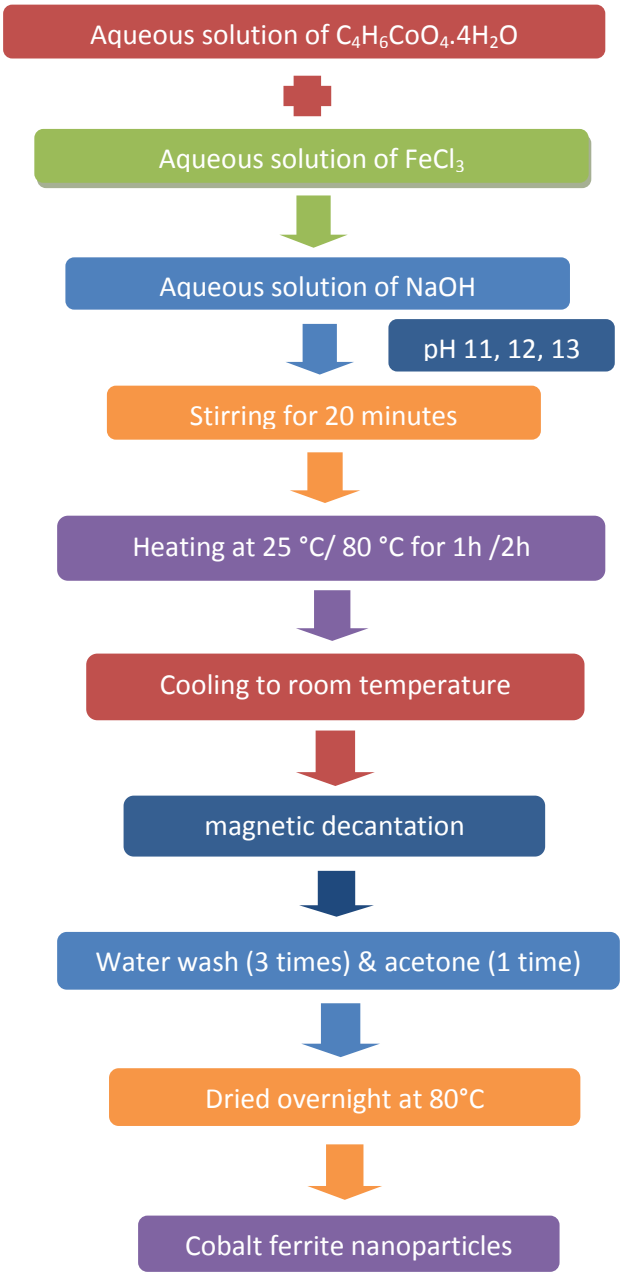

Figure 3.1: Synthesis protocols followed for the preparation of cobalt ferrite nanoparticles

3.2.1 X-Ray Diffraction (XRD)

X-rays are the rays like other electromagnet rays that can be diffracted. Diffraction means bending of light around the corners of an obstacle. The size of an obstacle should be comparable to wavelength of x-rays for observable diffraction. X-ray

diffraction is a technique which is used to find the structure of crystalline material and atomic spacing. The material should be fine powdered and homogenized. For determination of crystallinity, the XRD is the fastest and easy process. X-rays are the electromagnetic radiations and wavelengths from few angstroms to 0.1 angstroms are used for diffraction. X-ray diffraction is based on constructive interference of crystalline material and monochromatic x-rays. The electrons are produced by heating a filament in cathode ray tube (CRT) to produce the X-rays. Wavelength of x-rays should be comparable to size of atoms to find the structure. Powder diffraction is widely used in x-ray diffraction. The sample for characterization with powder diffraction method is in powder form. These x-rays are filtered to get a monochromatic radiation and then directed towards the sample. To bombard target material with electrons, accelerate the electrons towards the target by applying voltage. X-ray spectra are produced when electrons have sufficient energy to eject electrons from inner shell of the target material. X-rays are used to measure size, shape of the sample. It is used to find the orientation of the sample. To find the crystallite size Debye-scherrer method is used [43].

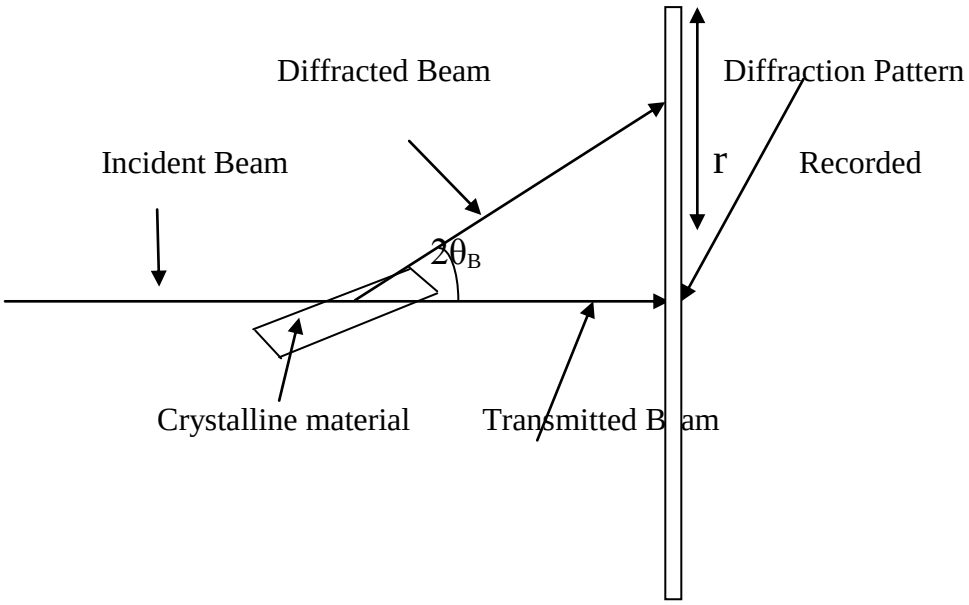

Figure 3.2: Schematic diagram of X-ray Diffraction experiment

Debye-Scherrer Formula

$$d_c = k\lambda/\beta\cos\theta$$

Where, k = Scherrer Constant, λ = wavelength of incident x rays, β = Full Width at half Maxima of a diffraction peak. To find the interplanar spacing we use Bragg's law. The schematic representation of X-ray diffraction from set of lattice planes is shown in figure 3.3

$$2d\sin\theta = n\lambda$$

Where, d = Interplanar spacing, θ = diffraction angle, λ = wavelength of incident X-rays and n is order of diffraction.

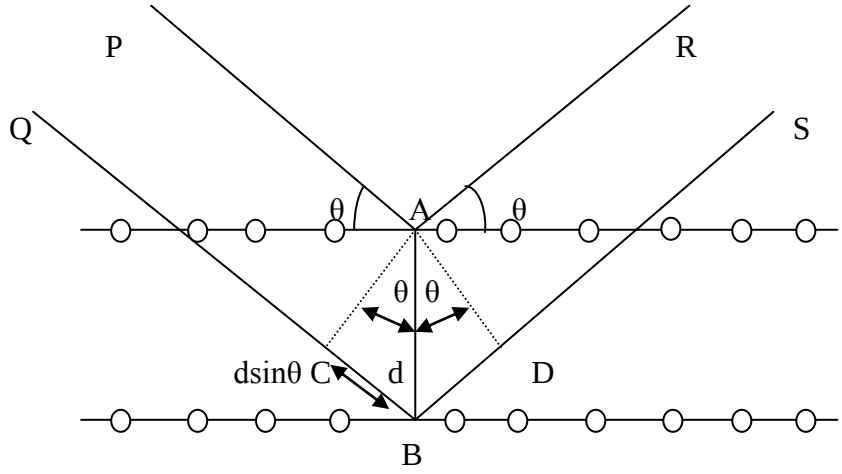

Figure 3.3: Schematic representation of X-ray diffraction from lattice planes

3.2.2 Vibrating Sample Magnetometer

VSM is vibrating sample magnetometer which is most convenient and beneficial magnetometer for the measurement of magnetic properties of magnetic materials. The principle of VSM is based on Faraday's law which tells that an electromagnetic force is induced in coil when flux is changed through the coil. Electric field is produced with the change in magnetic field. This electric field tells us about changing in magnetic field. In VSM, the material is placed in the uniform magnetic field (H) and magnetic moment (emu) will be induced in the material. Sample starts vibrating mechanically when placed in sensing coils due to magnetic field. Due to the change in magnetic flux voltage will be induced that equal to the magnetic moment of the sample. The domains are aligned when magnetic particles are magnetized by applied field. Stronger the magnetic field, the larger the magnetic moment will be. The magnetic moment of the sample will create a magnetic field around the sample. The hysteresis loop showed that the information about magnetic properties of the sample like saturation magnetization (M_s), remanant magnetization (M_r) and the coercivity (H_c) can be determined from VSM measurements [44]. The schematic diagram of typical vibrating sample magnetometer is shown in figure 3.4.

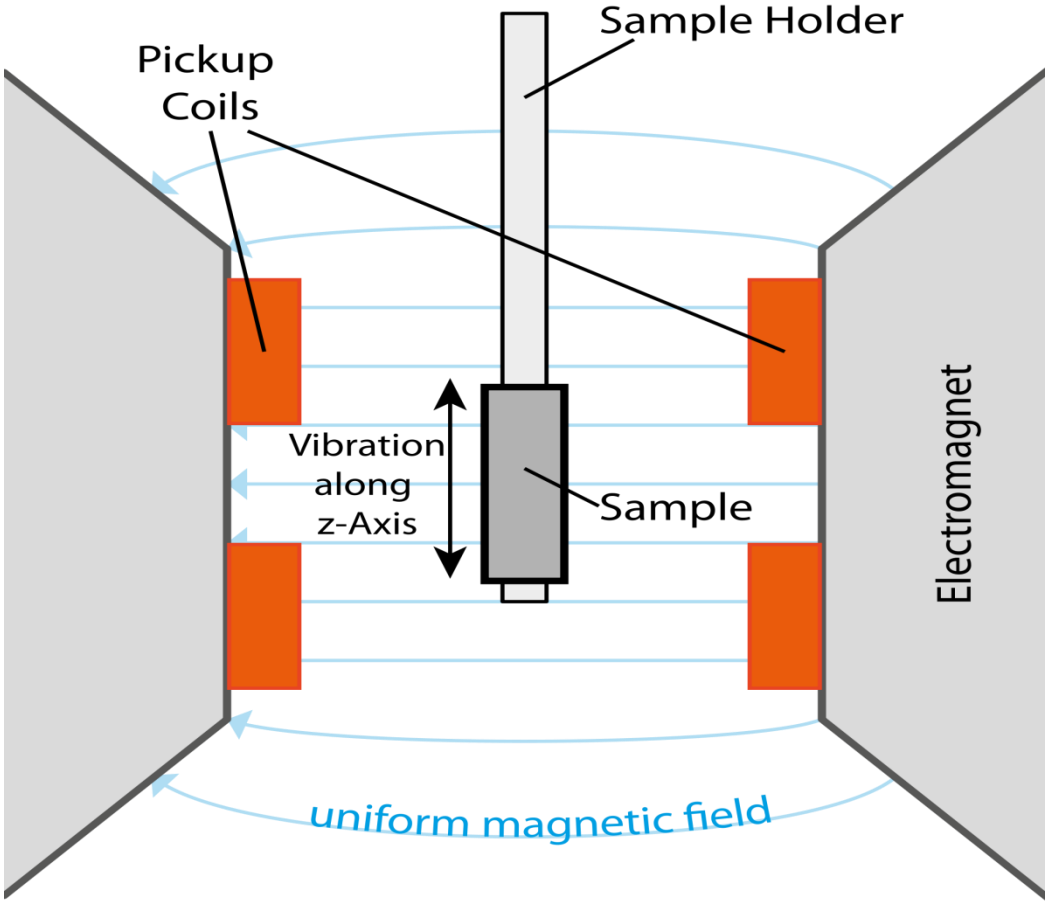

Figure 3.4: Schematic representation of vibrating sample magnetometer

3.2.4 Differential scanning calorimetry (DSC)

In DSC, heat flows through sample and reference. The temperature of sample and reference is same for the whole experiment. To maintain the temperature difference zero between the sample and reference, amount of energy has to be supplied or withdrawn from the sample. The sample and reference are placed in metal pans or individual base which contains heater and platinum resistance thermometer. An empty pan is used as reference. Compare the temperature of two thermometers and to remain the temperature equal, electric power is supplied to heater. If there is exothermic changes occur in sample, the heat supplied to the reference is more as compared to sample. If endothermic changes occur in sample then more heat has to be supplied to the sample heater. The difference in energy supplied to the sample and reference is noted as a function of temperature. The heat is required to change the sample temperature is determined by the signal i.e. proportional to specific heat of sample. The variation in the power signal is produced by change in specific heat that results in transition. The change of enthalpy of the sample tells us about area of the peak and direction of peak tells us about the processes i.e. exothermic or endothermic. Based on

this, if magnetic sample is kept for DSC measurement, a Curie point of the sample can be measured as at Curie point either the heat will be evolved or absorbed by the sample as this is an ordered- disordered transition.

Figure 3.5: Schematic representation of Differential scanning calorimeter

3.2.3 Transmission Electron Microscopy (TEM)

TEM is a microscopy technique in which electron beam is transmitted through an ultra thin specimen, interacting with the specimen as it passes through. When the beam is transmitted through the sample, it interacts with the electrons then the image is formed. This magnified image is focused on the device such as fluorescent screen or on a photographic film. When high energy beam transmitted through thin films to get the image as a result we get microstructure of materials with high resolution. At potential 40 to 100 kV a monochromatic beam is accelerated and then passed through strong magnetic field. Due to scattering of electrons, the image appears dark in the denser part. Diffraction contrast exhibit by scattering occurred from crystal planes. This diffraction contrast depends on the orientation of crystalline surface.

The TEM operates on the principle as the light microscope but electrons are used instead of light. Because electrons have smaller wavelength compared to light. The resolution of TEM images is much better than light microscope. The TEM specimen must be thin to transmit sufficient electrons to get image with minimum loss. The resolution of typical transmission electron microscope is 0.2 nm. We can find size, shape and arrangement of particles i.e. morphology of the sample and dimensions of nano materials. It tells us about structural order i.e. the sample is crystalline, polycrystalline or amorphous [43].

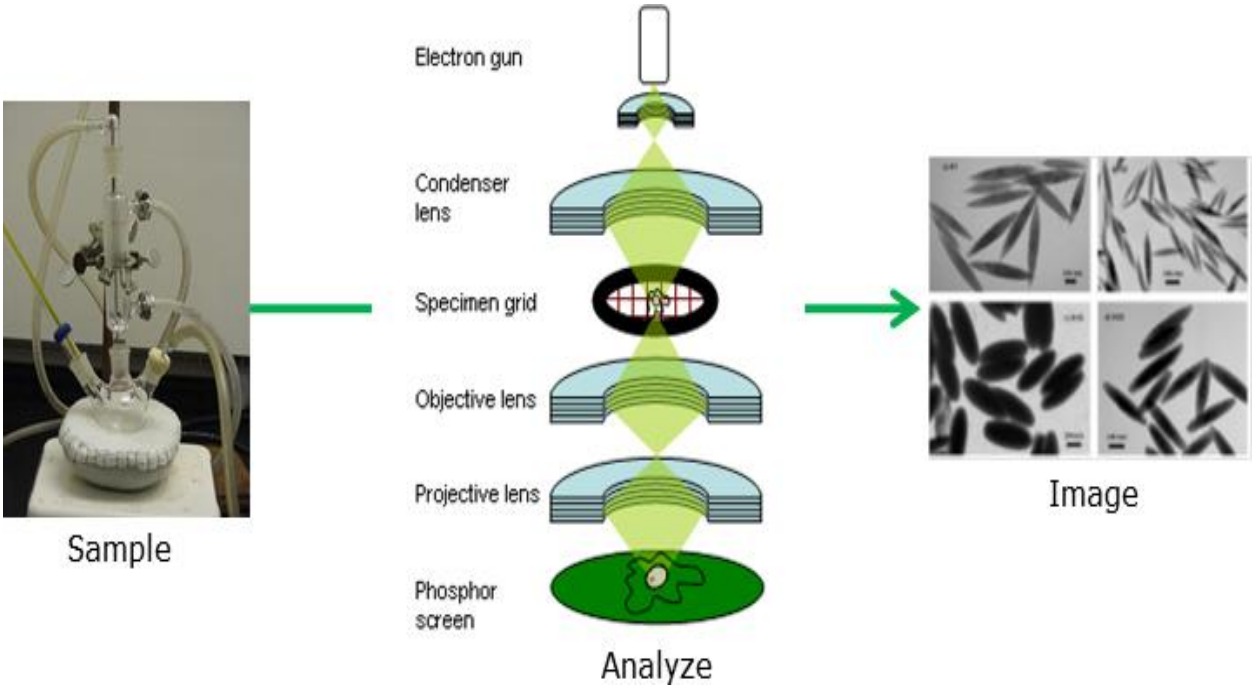

Figure 3.6: Schematic representation of Transmission electron microscope

CHAPTER 4

Results and Discussions

4.1 X-Ray Diffraction

Nanoparticles of cobalt ferrite are prepared by changing the parameters such as reaction pH, reaction temperature and reaction time. Samples are further characterized by XRD. The XRD data is collected at room temp in the range of $25° \leq 2\theta \leq 80°$ by using monochromatic CuKα radiation having wavelength 1.54 Å [21].

Three series of samples are prepared at various pH to examine the crystallite size of cobalt ferrite nanoparticles. First series of samples are prepared at room temperature by varying pH from 11 to 13 and peak broadening is found to be at an angle of $2\theta \sim 35.29°$. XRD pattern of cobalt ferrite nanoparticles prepared at room temperature and 80 °C are shown in figure 4.1, 4.3, 4.5 respectively. Diffraction peaks are indexed well with the inverse spinel structure. The crystallite size of nanoparticles prepared at room temperature varies in the range of 9 to 14 nm. Variation in the crystallite size of nanoparticles as a function of reaction pH is also shown in figure 4.2, 4.4, 4.6 respectively. Trend is in good agreement with those reported in literature. Second series of samples are prepared at 80°C for 1h with variation in pH from 11 to 13. The crystallite size of samples varies in the range of 8 to 13 nm. Third series of samples are prepared at 80°C for 2h with pH variation from 11 to 13. The crystallite size is found to be in the range of 8 to 14 nm. Cobalt ferrite nanoparticles show inverse spinel structure [37, 45].

Table 4.1: Crystallite Size of cobalt ferrite nanoparticles prepared at 25 °C/80°C for 1h and 2h

Condition	pH	Crystallite Size (nm)
20 min @25°C	11	10.76
	12	9.33
	13	14
1h Heating @ 80 °C	11	12.72
	12	8.75
	13	11.66
2 h Heating @80 °C	11	8.75
	12	14
	13	12.17

The crystallite size is determined from most intense peak by using scherrer method i.e.

$$d_{hkl} = k\lambda/\beta\cos\theta$$

Where λ is wavelength of radiation, θ is the angle of diffraction, β is FWHM, d_{hkl} is the crystallite size [29]. The results are summarized in table 4.1. They are also in good agreement with those reported in literature.

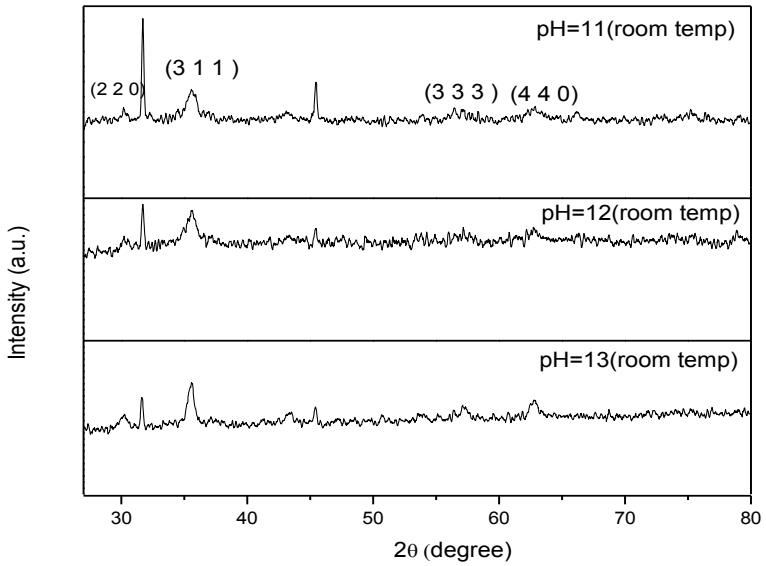

Figure 4.1: XRD Pattern of cobalt ferrites are prepared at 25 °C as a function of pH

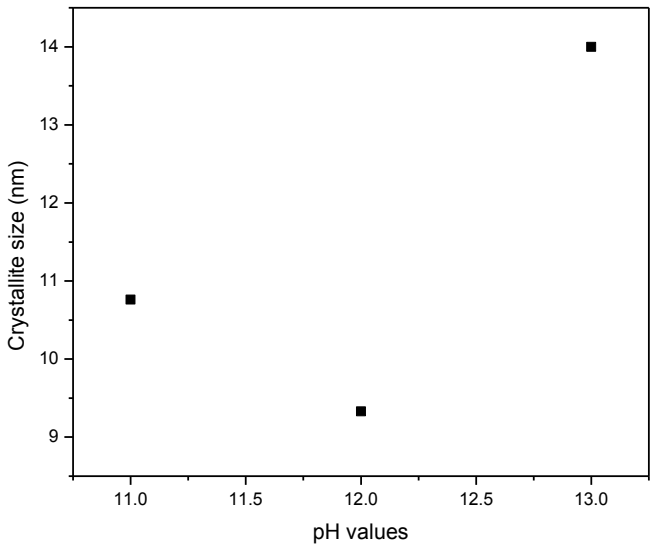

Figure 4.2: Crystallite size variation of nanoparticles prepared at room temperature as a function of reaction pH

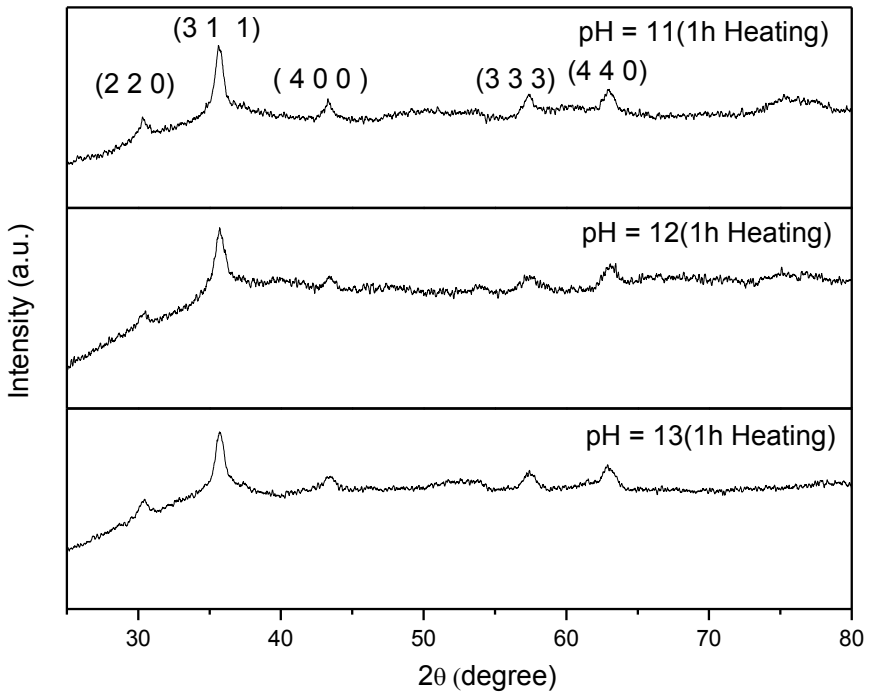

Figure 4.3: XRD Pattern of cobalt ferrites prepared at 80 °C as a function of pH

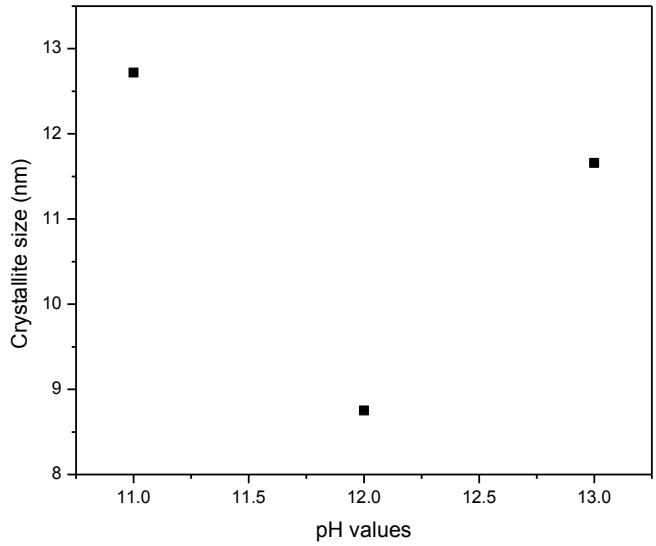

Figure 4.4: Crystallite size variation of nanoparticles prepared as a function of reaction pH

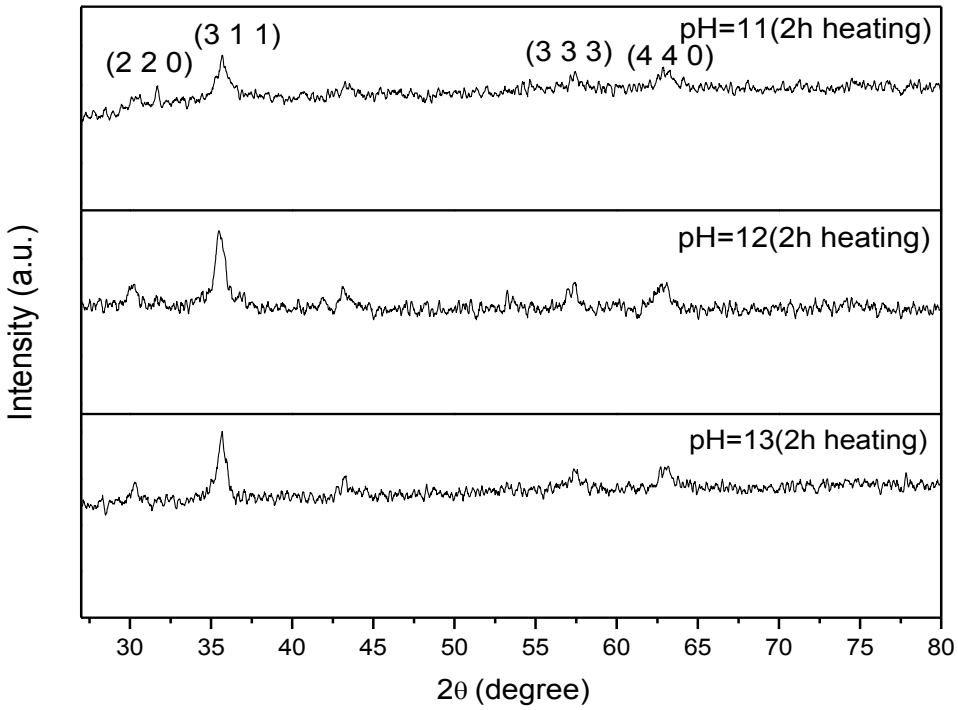

Figure1: XRD pattern of cobalt ferrites prepared at 80 °C as a function of pH

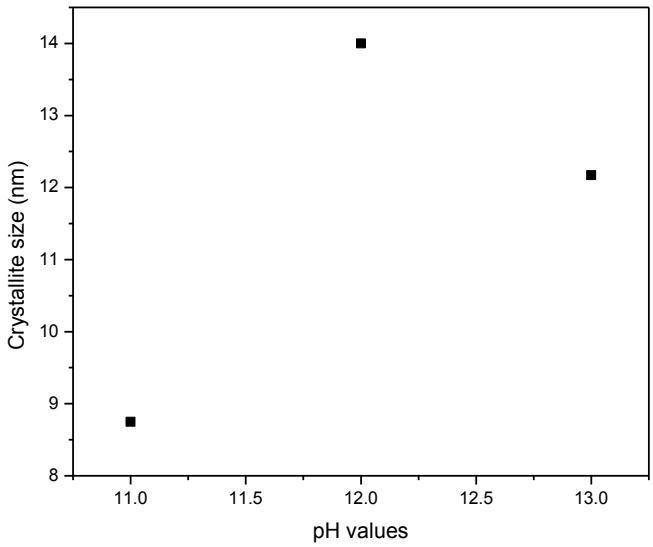

Figure 4.6: Crystallite size variation of nanoparticles prepared as function of reaction pH

4.2 Vibrating Sample Magnetometer

The magnetization curve(M-H) of cobalt ferrite nanoparticles is measured using Lake Shore VSM at room temperature. Magnetic behavior of the particles such as saturation magnetization depends on the method of synthesis. The hysteresis loop shows magnetization versus magnetic field upto 10,000 Oe at room temperature. Saturation magnetization is the maximum magnetize, at a field does not increase further with the increase in magnetic field. Saturation magnetization of the samples varies from 15 to 35 emu/g. The value of M_s of nanoparticles is smaller than the bulk materials [29]. Saturation magnetization for First series of samples are prepared at room temperature is found to be 19.11, 15.24, 20.55 emu/g. For second series of samples, saturation magnetization of samples prepared at 80°C for 1h is found to be 35, 22.28, 28.51 emu/g. For Third series of samples, Saturation magnetization of samples prepared at 80°C for 2h is found to be 15.58, 31.35, 23.93 emu/g. The highest value of saturation magnetization is 35 emu/g which is obtained when sample is prepared by 1h heating at pH 11. It is observed that the saturation magnetization decreases with decrease in particle size. Similar trend was found by Zhang et al. [29]. Field required to demagnetize the sample is known as coercive field. From hysteresis loop we observed that the coercivity of samples is ranging from 170 to 640 Oe. The value of magnetization after the removal of magnetic field is known as remanence. The remanent magnetization of these samples is found to be in the range of 2.84 - 8.57 emu/g. No specific trend in the variation in saturation magnetization, coercivity and remanence is observed as a function of reaction pH, reaction temperature and reaction time. However, with increase in particles, these parameters do increases, which is in good agreement with already reported literature.

Table 4.2: Magnetic properties of cobalt ferrite nanoparticles prepared at 25 °C/80°C for 1h and 2h

Heating	PH	M_s (emu/g)	H_c (Oe)	M_r (emu/g)
Room Temperature	11	19.11	174.62	2.90
	12	15.24	235.94	2.84
	13	20.55	515.88	6.05
1h Heating	11	35	341.03	8.46
	12	22.28	278.82	4.84
	13	28.51	429.90	8.30
2h Heating	11	15.58	641.52	4.28
	12	31.35	480.44	8.57
	13	23.93	553.21	6.28

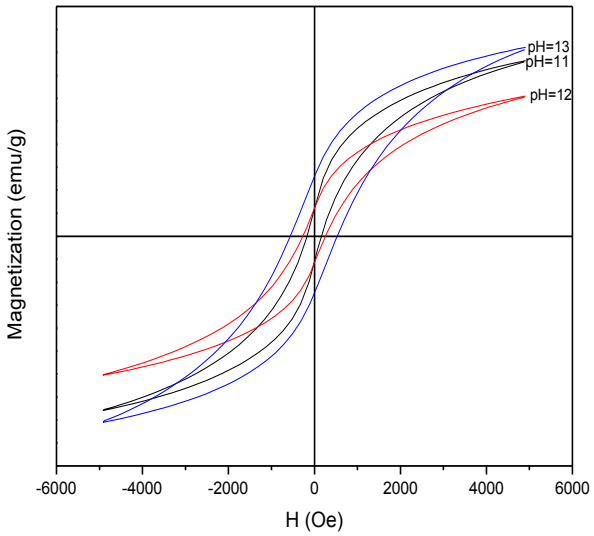

Figure 2.7: Magnetization curves at Room Temperature with pH variation

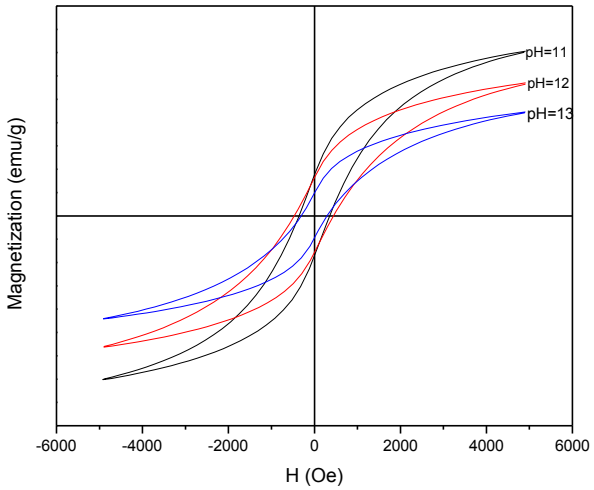

Figure 4.8: Magnetization curves at 1h Heating with pH variation

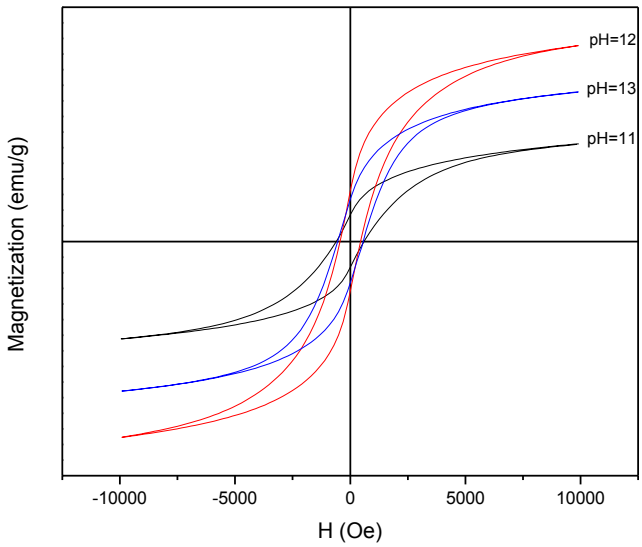

Figure 4.9: Magnetization curves at 2h Heating with pH variation

4.3 Differential Scanning Calorimetry

The DSC curve of cobalt ferrite nanoparticles which are prepared at 80 °C temperature for 1h and 2h is shown in Figure 4.10, 4.11 respectively. The DSC curve shows endothermic and exothermic peaks from room temperature to 600°C temperature. Curie temperature of second series of Samples is found to be 311.79 °C, 325.01 °C and 350.08 °C respectively. For third series of samples, Curie temperature is found to be 319.01 °C, 307.02 °C and 340.54 °C. In some cases, the transition is very weak but still observable. Curie temperatures could not be measured for series of samples prepared at room temperature.

Table 4.3: Curie temperature of cobalt ferrite nanoparticles prepared at 80°C for 1h and 2h

Conditions	pH	Curie Temperature (°C)
1h Heating	11	311.79
	12	325.01
	13	350.08
2h Heating	11	319.01
	12	307.02
	13	340.54

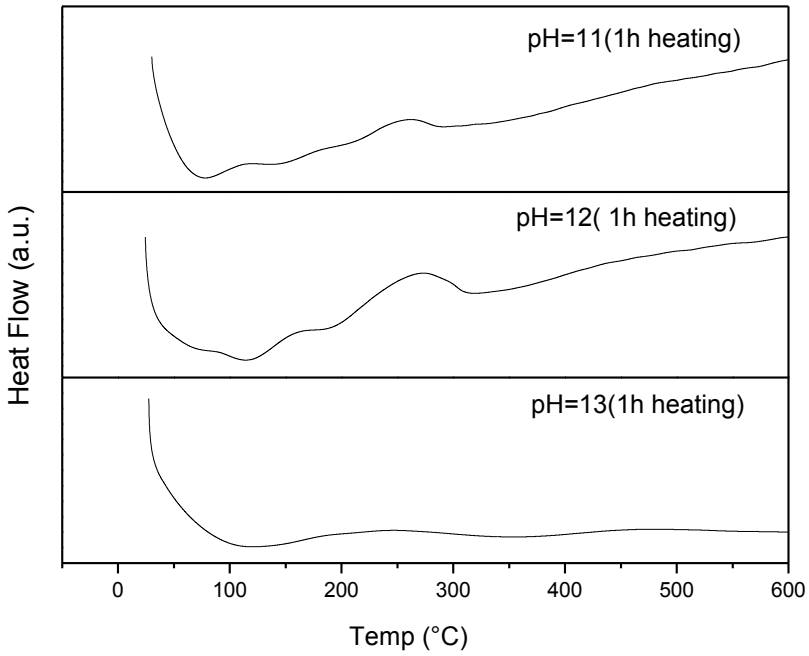

Figure 4.10: DSC curve of cobalt ferrite nanoparticles prepared at 80 °C for 1h

Heating

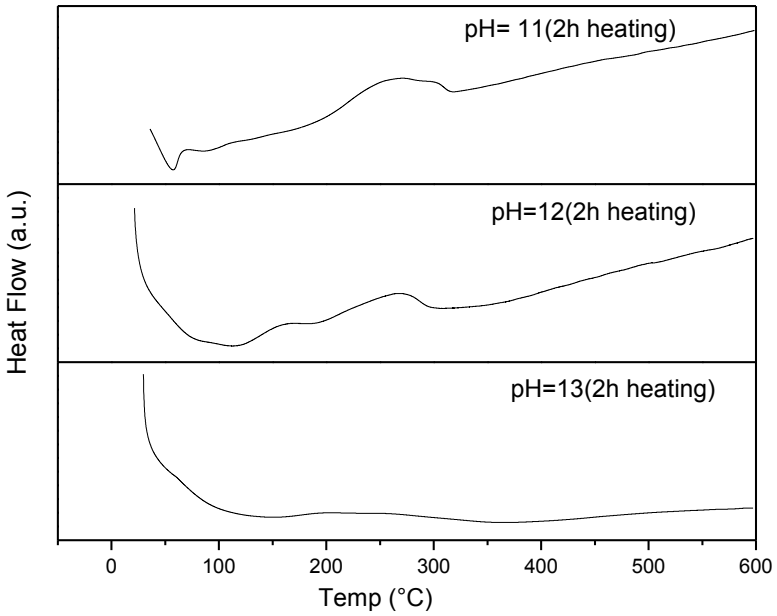

Figure 4.11: DSC curve of cobalt ferrite nanoparticles prepared at 80 °C for 2h heating

4.4 Transmission Electron Microscopy

Transmission electron microscopic image of cobalt ferrite nanoparticles prepared at pH 11 for heating period of 1h @ 80 °C is shown in figure 4.12. Well dispersed nanoparticles with near spherical morphology can be observed in the TEM micrograph. The size distribution histogram of nanoparticles is also prepared and shown in figure 4.12. The histogram is fitted with lognormal size distribution function. The mean physical size was 11.50 nm and polydispersity index is 0.25. These results are in good agreement with those found in literature for ferrite nanoparticles.

Table 4.4: Physical size of cobalt ferrite nanoparticles prepared at 80°C for 1h

Heating	pH	Physical size (nm)
1h Heating	11	11.49

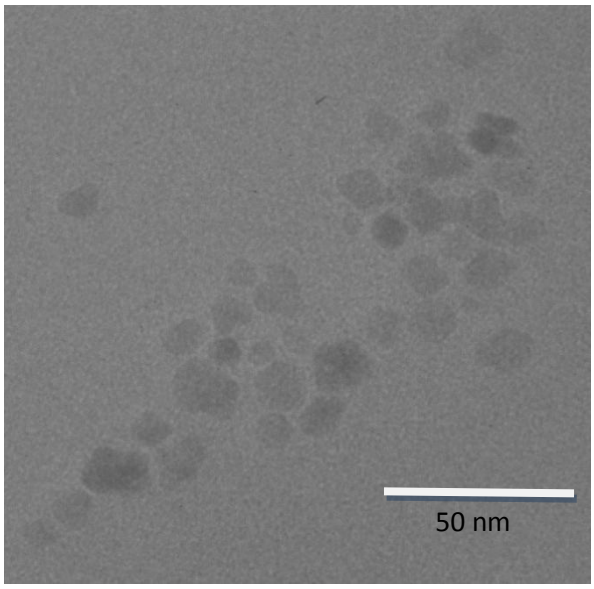

Figure 4.12: TEM image of Cobalt Ferrite at 1h heating with pH 11

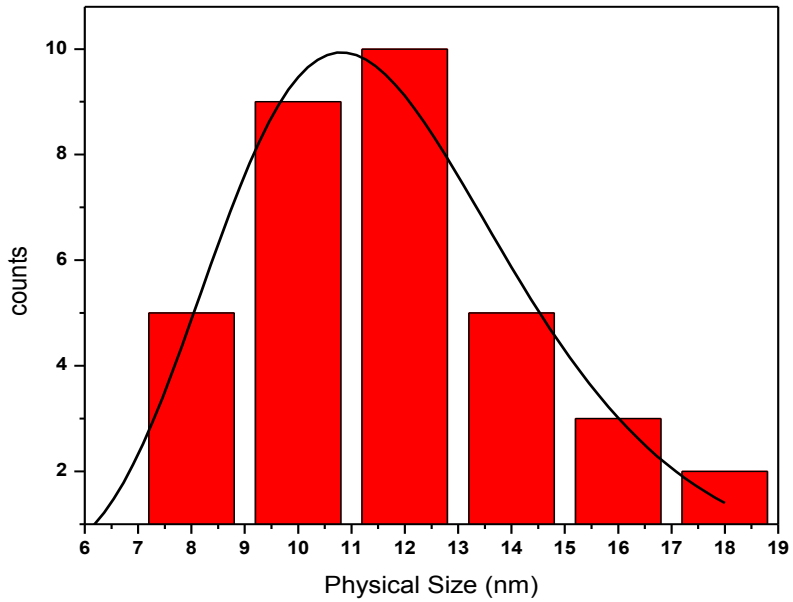

Figure 4.13: Average size distribution of Cobalt Ferrite nanoparticles by TEM

Conclusions

Cobalt ferrite nanoparticles have been synthesized by chemical co-precipitation technique; the variables of the study were reaction pH, reaction time and reaction temperature. From x-ray analysis, it has been found that nanoparticles in each case crystallites into inverse spinel structure. No specific trend in crystallite size variation was observed as a function of reaction pH, reaction temperature and time. The crystallite size was observed to vary between 9-14 nm. Magnetic characteristics (saturation magnetization, coercivity, remanence) do not show any systematic trend as a function of processing variables. However, they show a general trend of decrease with decreasing particle size. Nanoparticles are in ferrimagnetic state which transforms to paramagnetic state at a Curie temperature lying in the range of 307- 350 °C. Saturation magnetization, coercivity and remanence all remained quite low due to surface and quantum size effects.

References

[1] L. Filipponi, D. Sutherland, "*Nanotechnology" - A Brief Introduction* (2007)

[2] N. Lane, *"Nano Research*"**,3**(2005)95

[3] C. Suryanarayana, *"Nanomaterials"*, **54**(2002)24

[4] B. Issa, I. M. Obaidat, B. A. Albiss, Y. Haik, *"Molecular Science"*, **14**(2013)21266

[5] V. Raghavan, *"Materials Science and Engineering(PHI Learning Private Limited, Fifth Edition)"*, (2010)

[6] F. Gazeau, J. C. Bacri, F. Gendron, R. Perzynski, Y. L. Raikher, V. I. Stepanov, E. Dubois, *"Magnetism and Magnetic Materials"*, **186**(1998)175

[7] A. H. Lu, E. L. Salabas, F. Schuth, *"Magnetic Nanoparticles"*Wiley-VCH verlagGmbh& Co. KGaA, Weinheim, (2007)1223

[8] B. N. Pianciola, E. L. Jr., H. E. Troiani, L. C. C. M. Nagamine, R. Cohen, R. D. Zysler, *"Magnetism and Magnetic Materials"* **377**(2015)44

[9] J. Bowles, M. Jackson, A. Chen, P. Solheid, *"The IRM Quarterly"* **19**(2009)3

[10] M. Marolt, *"Superparamagnetic Materials"*, (2014)

[11] M. Benz, *"Superparamagnetism: Theory and Applications"*,(2012)

[12] M. Houshiar, F. Zebhi, Z. J. Razi, A. Alidoust, Z. Askari, *"Magnetism and Magnetic Materials"*, **371**(2014)43

[13] M. Mozaffari, J. Amighian, E. Darsheshdar, *"Magnetism and Magnetic Materials"*, **350**(2014)19

[14] M. Meshram, N. K. Agarwal, B. Sinha, P. S .Mishra, *"Magnetism and Magnetic Materials"*, **271**(2004)207

[15] K. Maaz, G. H. Kim, *"Materials Chemistry and Physics"*, **137**(2012)359

[16] A. B. Gadkari, T. J. Shinde, P. N. Vasambekar, *"Materials Chemistry and Physics"*, **114**(2009)505

[17] M. A. Ahmed, A. A. E. Khawlani, *"Magnetism and Magnetic Materials"*,**329**(2009)1959

[18] L. Kumar, P. Kumar, A. Narayan, M. Kar, *"International Nano Letters"*, **3**(2013)8

[19] S. Rana, J. Philip, B. Raj, *"Materials Chemistry and Physics"*, **124**(2010)264

[20] K. Maaz, A. Mumtaz, S. K. Hasanain, A. Ceylan, *"Magnetism and Magnetic Materials"*, **308**(2007)289

[21] C. Fei, Y. Zhang, Z. Yang, Y. Liu, R. Xiong, J. Shi, X. Ruan, *"Magnetism and Magnetic Materials"*, **323**(2011)1811

[22] F. S. Li, L. Wang, Q. G. Zhou, X. Z. Zhou, H. P. Kunkel, G. Williams, *"Magnetism and Magnetic Materials"*, **268**(2004)332

[23] A. B. Shinde, *"Innovative Technology and Exploring Engineering"*, **3**(2013)2278

[24] C. Liu, B. Zou, A. J. Rondinone, Z. J. Zhang, *"American Chemical Society"*, **122**(2000)6263

[25] I. Sharifi, H. Shokrollahi, M. M. Doroodmand, R. Safi, *"Magnetism and Magnetic Materials"*, **324**(2012)1854

[26] M. G. Naseri, E. B. Saion, H. A. Ahangar, A. H. Shaari, M. Hashim, *"Nanomaterials"*, DOI:10.1155/2010/907686
[27] A. Franco, V. Zapf, *"Magnetism and Magnetic Materials"*, **320**(2008)709
[28] Y. Zhang, Z. Yang, D. Yin, Y. Liu, C. Fei, R. Xiong, J. Shi, G. Yan, *"Magnetism and Magnetism Materials"*, **322**(2010)3470
[29] Z. Zi, Y. Sun, X. Zhu, Z. Yang, J. Dai, W. Song, *"Magnetism and Magnetic Materials"*, **321**(2009)1251
[30] Y. Kim, D. Kim, C. S. Lee, *"Physica B"*, **337**(2003)42
[31] N. Hanh, O. K. Quy, N. P. Thuy, L. D. Tung, L. Spinu, *"Physica B"*, **27**(2003)382
[32] E. J. Choi, Y. Ahn, S. Kim, D. H. An, K. U. Kang, B. G. Lee, K. S. Baek, H. N. Oak, *"Magnetism and Magnetic Materials"*, **262**(2003)198
[33] C. N. Chinnasamy, M. Senoue, B. Jeyadevan, O. P. Perez, K. Shinoda, K. Tohji, *"Colloid and Interface science"*, **263**(2003)80]
[34] L. Zhao, H. Zhang, Y. Xing, S. Song, S. Yu, W. Shi, X. Guo, J. Yang, Y. Lei, F. Cao, *"Solid State Chemistry"*, **181**(2008)245
[35] B. G. Toksha, S. E. Shirsath, S. M. Patange, K. M. Jadhav, *"Solid State Communications"*, **147**(2008)479
[36] S. Y. Vilar, M. S. Andujar, C. G. Aguirre, J. Mirra, *"Solid State Chemistry"*, **182**(2009)2685
[37] R. M. Mohamed, M. M. Rashad, F. A. Haraz, W. Sigmund, *"Magnetism and Magnetic Materials"*, **322**(2010)2058
[38] M. M. E. Okr, M. A. Salem, M. S. Salim, R. M. E. Okr, M. Ashoush, H. M. Talaat, *"Magnetism and Magnetic Materials"*, **323**(2011)920
[39] S. Briceno, W. B. Escamilla, P. Silva, G. E. Delgado, E. Plaza, J. Palacios, E. Canizales, *"Magnetism and Magnetic Materials"*, **324**(2012)2926
[40] E. Mazario, P. Herrasti, M. P. Morales, N. Menendez, *"Nanotechnology"*, **23**(2012)355708
[41] F. Huixia, C. Baiyi, Z. Devi, J. T. Lin, *"Magnetism and Magnetic Materials"*, **356**(2014)68
[42] K. Hedayati, S. Azarakhsh, D. Ghanbari**,** *"DOI:10.7508/jns.2016.02.004"***(**2016)125
[43] G. A. Dorofeev, A. N. Streletskii, I. V. Povstugar, A. V. Protasov, E. P. Elsukov, *"Colloid"*, **74**(2012)675
[44] S. Kelutia, L. Saneblidze, V. Mikelashvili, J. Markhulia, R. Tatarashvili, D. Daraselia, D. Japaridze, *"Synthesis of Nanoparticles for Biomedical Applications"*, **4**(2015)33
[45] S. Dey, S. K. Dey, S. Majumder, A. Poddar, P. Dasgupta, S. Banerjee, S. Kumar, *"Physica B"*, **448**(2014)247